Composites Science and Technology **39** (1990) 63–74

Snap Buckling of Delaminated Composites under Pure Bending

G. A. Kardomateas

School of Aerospace Engineering, Georgia Institute of Technology, Atlanta, Georgia 30332-0150, USA

(Received 29 June 1989; accepted 23 November 1989)

ABSTRACT

Delaminated composites under pure bending can undergo snap buckling under certain conditions of applied bending load and geometrical configuration. The phenomenon is demonstrated experimentally and is investigated theoretically by an energy procedure. The geometric non-linearities are included in the formulation. First, a theoretical analysis is performed to model the behavior of the system and define the conditions for snap buckling. The predicted buckling loads are then compared with experimentally obtained data from pure bending loading of Kevlar epoxy specimens with internal delaminations. Good agreement is obtained between the experimental and theoretical results.

INTRODUCTION

When the application of layered composites or laminates to engineering components is contemplated, it is essential to answer not only the fundamental questions on the strength and stiffness of the material, but also the question of damage tolerance, i.e. the behavior of the system in the presence of defects. Indeed, the manufacture of composites requires involved procedures which may result in the existence of defects in the finished product.[1] Delaminations or interlayer cracks may also result from events during service life such as when objects traveling at low velocity strike composite laminated plates.[2] As a consequence, structural elements with delaminations under compression suffer a degradation of their buckling

Composites Science and Technology 0266–3538/90/$03·50

strength and potential loss of integrity from possible growth of the interlayer crack. Delamination buckling under compression has received considerable attention,[3-8] and numerous studies have addressed related issues in both one-dimensional and two-dimensional treatments.[9,10] However, practical configurations involve loading of composite components not only in pure compression but also in bending. For example, bending is the normal service load for the members of composite beam frame systems or the load introduced from longitudinal impact of non-straight composite beams.[5] Therefore, it is of particular interest to study the behavior of laminated components with delaminations under bending.

Let us consider the delaminated composite beam of Fig. 1 subjected to four-point bending. The resulting state of pure bending will introduce at the sections adjacent to the delamination tip an effective compressive force at the upper part and an equal tensile force at the lower part. Under this compressive loading the upper delaminated part may buckle, after an initial bending deformation. Subsequent growth of the delamination may follow the instability point. This problem differs fundamentally from the usual case of buckling under compression, where the equilibrium form after buckling is close to the equilibrium form before buckling. This is because of the induced initial bending deformation which makes the transition to a new equilibrium state occur by a snap, and the new equilibrium form to differ essentially from the initial one. On this subject there has been only an analytical study for the case of a circular delamination in a plate under axisymmetric compression and bending.[11]

The object of this paper is to present not only a formulation and solution for the problem of snap-through buckling of beam/plates with through-width delaminations but also experimental data on this phenomenon. The

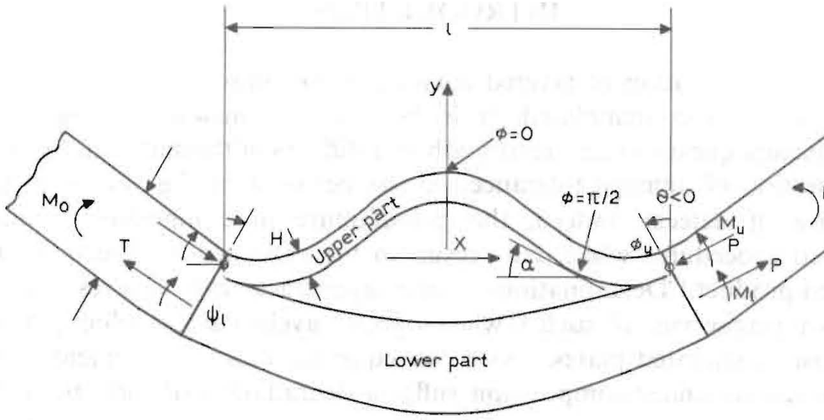

Fig. 1. Definition of the geometry and of the quantities involved in the non-linear model for the post-buckled shape.

problem is non-linear, and large deflection equations will be used in the formulation. The test results will be from experiments on unidirectional Kevlar/epoxy specimens.

ANALYSIS

Let us consider a homogeneous, orthotropic beam-plate of thickness T and of unit width containing a delamination at a depth H ($H \leq T/2$) from the top surface of the plate. The beam is subjected to bending moments M_0. As shown in Fig. 1, the interlayer crack extends over the interval $-l/2 \leq x \leq l/2$. The whole structure undergoes bending deformation. At the critical value of bending moment the delaminated layer snaps out. Thus there is a fundamental difference from the usual case of compressed members in which the delaminated layer bifurcates from a membrane state (state of pure compression) to the buckled state. In the present case of bending loading, a pure membrane state is absent, and separation occurs abruptly and in a discontinuous manner, with a resulting snap-through of the delaminated layer.

In systems that exhibit snap buckling, the energy criterion has been used extensively.[11–13] As no energy is transferred to the system during the snap, but some may be lost, it can only be expected that the system jumps from a state of higher energy to a state of lower energy. If no energy is lost, the minimum load at which a snap can occur is then the load at which the total energy in the buckled and unbuckled states are equal.[14] As an alternative formulation, which should lead to an exact solution, we would have to solve the governing differential equations and obtain the corresponding load–deflection curve. Such an approach is extremely difficult, however, because it should incorporate the initial deflections and the appropriate stresses and deformations that exist in the pre-buckling state in the different constituent parts of the system. Therefore, because of the simplicity offered by the energy criterion, this approach will be used here.

The post-buckled shape is shown in Fig. 1. Over the region of the delamination the beam consists of two parts: the delaminated layer (upper part, of thickness H) and the part below the delamination (lower part, of thickness $T-H$). To describe the deformation of each constituent part, taking the geometric non-linearities into account, we use the exact theory of plane deformation of members that are restrained elastically at the ends by means of concentrated forces and moments. However, the first important observation is that, owing to the bending loading, the two parts have an essential difference, as the upper buckled layer is part of a compressive elastica with inflection points whereas the lower part is part of a non-inflectional tensile curve.

To describe the deformation of the delaminated layer, which is part of an inflectional compressive elastic curve, two variables play an important role: the end-amplitude for the compressed film, Φ_u and the distortion parameter, α, which is the angle of tangent rotation at the inflection point from the straight position.[15] These are the generalized coordinates of deformation. In the buckled form, which is assumed to be symmetrical, we denote the end forces and moments by P_u and M_u. In the following equations the quantities at the right end are used (see Fig. 1). The moments and angles are assumed positive clockwise. In terms of these two quantities, relations between the end stress resultants, P_u, M_u, as well as other coordinates of deformation such as end-slope, θ, and total flexural contraction, e_u, can be found. The relations require the use of elliptic integrals. We define

$$k = \sin(\alpha/2) \tag{1}$$

The first elliptic integral $F(\Phi, k)$ is defined by

$$F(\Phi, k) = \int_0^{\Phi} \frac{d\phi}{\sqrt{(1 - k^2 \sin^2 \phi)}} \tag{2a}$$

and the second elliptic integral by

$$E(\Phi, k) = \int_0^{\Phi} \sqrt{(1 - k^2 \sin^2 \phi)}\, d\phi \tag{2b}$$

The values of those integrals at the end $F(\Phi_u, k)$, $E(\Phi_u, k)$ are of most interest. We denote by D_i the bending stiffness of each constituent part (upper or lower), $D_i = Et_i^3/[12(1 - \nu_{13}\nu_{31})]$, t_i being the thickness of the corresponding part and E the modulus of elasticity along the $x \equiv 1$ axis. The following five relations define the characteristics of the post-buckled delaminated layer:[15]

Axial force

$$P_u = P = 4D_u F^2(\Phi_u, k)/l^2 \tag{3a}$$

Moment at right end

$$M_u = 4(D_u/l)kF(\Phi_u, k)\cos\Phi_u \tag{3b}$$

Rotation at right end

$$\theta_u = \theta = 2\arcsin(k \sin\Phi_u) \tag{3c}$$

Flexural contraction

$$\lambda_u = e_u/l = 2\left[1 - \frac{E(\Phi_u, k)}{F(\Phi_u, k)}\right] \tag{3d}$$

Flexural elastic energy

$$U_u = 8(D_u/l)F(\Phi_u, k)[E(\Phi_u, k) - F(\Phi_u, k)\cos^2(\alpha/2)] \tag{3e}$$

Furthermore, the deflection at the middle, normal to the central line of thrust (direction of axial forces P_u), Y_{um} is found from

$$Y_{um} = 2k\sqrt{(D_u/P_u)}(1 - \cos\Phi_u) \tag{4a}$$

It should be noted that at each point x there corresponds a value of the variable Φ (amplitude for compressive members); the value at $x = l/2$ is Φ_u. Furthermore, at the inflection point, where the slope $\theta = \alpha$, the value is $\Phi = \pi/2$ and at the middle $x = 0$, where $\theta = 0$, $\Phi = 0$. With these remarks in mind, the deflections at all other points can now be obtained from

$$y_u(x) = 2k\sqrt{(D_u/P_u)}[\cos\Phi(x) - \cos\Phi_u] \tag{4b}$$

where $\Phi(x)$ is found from the implicit relation

$$F(\Phi(x), k) = 2F(\Phi_u, k)x/l \tag{4c}$$

To describe the deformation of the lower part, which is part of a non-inflectional tensile elastic curve, i.e. an elastic curve with curvature always of one sign, the generalized coordinates of deformation are the amplitude variable $\Psi(x)$ and the distortion parameter ε of tensile non-inflectional members.[15] The end stress resultants $P_l = P$ and M_l, as well as the end slope θ (same for both parts), the flexural contraction e_l and the energy U_l, are given by relations similar to (1)–(4). We define now the first elliptic integral $G(\Psi, \varepsilon)$ by

$$G(\Psi, \varepsilon) = \int_0^{\Psi} \frac{d\psi}{\sqrt{(1 - \sinh^2(\varepsilon/2)\sinh^2\psi)}} \tag{5a}$$

and the second elliptic integral for the tensile lower part by

$$H(\Psi, \varepsilon) = \int_0^{\Psi} \sqrt{(1 - \sinh^2(\varepsilon/2)\sinh^2\psi)}\, d\psi \tag{5b}$$

The value of the amplitude variable at the left end, denoted by Ψ_l and the corresponding values of the above integrals, $G(\Psi_l, \varepsilon)$ and $H(\Psi_l, \varepsilon)$ are of most interest (Fig. 1). The characteristic relations for the lower part are given as follows:

Axial force

$$P_l = P = 4D_l G^2(\Psi_l, \varepsilon)/l^2 \tag{6a}$$

Moment at left end

$$M_l = 4(D_l/l)G(\Psi_l, \varepsilon)\sinh\frac{\varepsilon}{2}\cosh\Psi_l \tag{6b}$$

Slope at left end

$$\theta_l = -\theta = 2\arcsin\left(\sinh\frac{\varepsilon}{2}\sinh\Psi_l\right) \tag{6c}$$

Flexural contraction

$$\lambda_l = e_l/l = 2\left[1 - \frac{H(\Psi_l, \varepsilon)}{G(\Psi_l, \varepsilon)}\right] \tag{6d}$$

Flexural elastic strain energy

$$U_l = 8(D_l/l)G(\Psi_l, \varepsilon)\left[G(\Psi_l, \varepsilon)\cosh^2\frac{\varepsilon}{2} - H(\Psi_l, \varepsilon)\right] \tag{6e}$$

Moments and angles are again assumed to be positive clockwise, so the values at the right end are of opposite sign. To obtain the deflections we integrate the relation for the slope $\phi(x)$ and the deflections $Y(x)$:

$$\mathrm{d}Y_l(x) = \sin\phi(x)\,\mathrm{d}x \tag{7a}$$

by using the following two expressions that are essential in deriving the theory of the tensile large displacement elastic curve:[15]

$$\sin^2\frac{\phi(x)}{2} = \sinh^2\frac{\varepsilon}{2}\sinh^2\Psi(x)$$

$$\frac{D_l}{P}\left(\frac{\mathrm{d}\Psi(x)}{\mathrm{d}x}\right)^2 = 1 - \sinh^2\frac{\varepsilon}{2}\sinh^2\Psi(x) \tag{7b}$$

Now, using the condition that at the end $x = -l/2$, $\Psi = \Psi_l$, we obtain the deflections from

$$Y_l(x) = 2\sinh\frac{\varepsilon}{2}\sqrt{(D_l/P_l)}\,[\cosh\Psi(x) - \cosh\Psi_l] \tag{7c}$$

where $\Psi(x)$ is found from the implicit relation

$$G(\Psi(x), \varepsilon) = 2G(\Psi_l, \varepsilon)x/l \tag{7d}$$

Furthermore, the deflection at the middle, $x = 0$, at which point $\Psi = 0$, is found from

$$Y_{lm} = 2\sinh(\varepsilon/2)\sqrt{(D_l/P_l)}(1 - \cosh\Psi_l) \tag{7e}$$

We now formulate the problem. The compressive end force at the upper delaminated part and the tensile end force at the lower part are equal due to the pure bending loading, resulting from (3a) and (6a):

$$H^3F^2(\Phi_u, k) - (T - H)^3G^2(\Psi_l, \varepsilon) = 0 \tag{8}$$

The deflections of the upper and lower parts should be geometrically compatible. Therefore an additional condition is derived from the compatible shortening of the upper and lower parts

$$(1-\nu_{13}\nu_{31})\frac{Pl}{w(T-H)E_1}+(1-\nu_{13}\nu_{31})\frac{Pl}{wHE_1}+e_u-e_l=T\theta \tag{9}$$

Substituting (3a), (3c), (3d) and (6d) into the above equation, we obtain

$$2\left[1-\frac{H(\Psi_l,\varepsilon)}{G(\Psi_l,\varepsilon)}\right]l-2\left[1-\frac{E(\Phi_u,k)}{F(\Phi_u,k)}\right]l-\frac{H^2TF^2(\Phi_u,k)}{3l(T-H)}-2T\arcsin(k\sin\Phi_u)=0 \tag{10}$$

The corresponding applied moment M_0 is found from a moment equilibrium at the common right end section (it should be noted that the moment at the right end for the lower part is of opposite sign from that in (3c)):

$$M_0=M_u-M_l+P(T/2) \tag{11a}$$

Substituting (3a), (3b) and (6b), we obtain

$$M_0=\frac{E}{3l(1-\nu_{13}\nu_{31})}\left[H^3kF(\Phi_u,k)\cos\Phi_u-(T-H)^3G(\Psi_l,\varepsilon)\sinh\frac{\varepsilon}{2}\cosh\Psi_l+TH^3F^2(\Phi_u,k)/(2l)\right] \tag{11b}$$

To be able to apply the energy criterion we need the expression for the total energy of the system. The total strain energy of the system is that due to both bending and compression or tension of the upper and lower parts:

$$U_{tot}=U_u+\frac{P_u^2l(1-\nu_{13}\nu_{31})}{2EH}+U_l+\frac{P_l^2l(1-\nu_{13}\nu_{31})}{2E(T-H)} \tag{12a}$$

where U_u, U_l are given by (3e) and (6e).

As the initial energy of the segment of length l and thickness T under pure bending is given by

$$U_0=6M_0^2l(1-\nu_{13}\nu_{31})/(ET^3) \tag{12b}$$

we have to fulfill the condition of

$$U_{tot}\le U_0 \tag{12c}$$

Therefore, in the limit of snap buckling,

$$\frac{2E}{3l(1-\nu_{13}\nu_{31})}\Bigg\{H^3F(\Phi_u,k)[E(\Phi_u,k)-F(\Phi_u,k)\cos^2(\alpha/2)] + (T-H)^3G(\Psi_l,\varepsilon)\left[G(\Psi_l,\varepsilon)\cosh^2\frac{\varepsilon}{2}-H(\Psi_l,\varepsilon)\right]+\frac{1}{12}\frac{TH^5F^4(\Phi_u,k)}{l^2(T-H)}\Bigg\} - 6M_0^2(\alpha,\varepsilon,\theta)\frac{l(1-\nu_{13}\nu_{31})}{EwT^3}=0 \quad (13)$$

where $M_0(\alpha,\varepsilon,\theta)$ is given by (11b).

Equations (8), (10) and (13) constitute a system of three non-linear equations that can be solved for the distortion parameters α and ε and the end slope θ.

In the solution procedure the end-amplitude values are found from (3c) and (6c) as follows. If arcsin gives the principal value, as $\pi < \Phi_u < 3\pi/2$, we obtain

$$\Phi_u = \pi - \arcsin[\sin(\theta/2)/\sin(\alpha/2)] \quad (14a)$$

$$\Psi_l = \ln(x+\sqrt{(x^2+1)}) \qquad x = -\sin(\theta/2)/\sinh(\varepsilon/2) \quad (14b)$$

The values of the functions F, E, G, H at these end-points are found from the elliptic integral definitions (2) and (5). Moreover, in the solution algorithm for a certain value of the slope θ, the search for the distortion parameter ε is for values from 0·01 to 0·50, whereas, in view of (11a), the search for the distortion angle α of the delaminated layer is for values from $|\theta|$ to 90°. There may be values of the slope θ for which a solution cannot be found, i.e. it is not possible to find α and ε that fulfill the compatibility condition (10). The point of snap buckling is defined as the first point (i.e. of minimum M_0 or $|\theta|$) for which a solution to the compatibility equation (10) exists and where the energy condition (12c) is fulfilled. The set of values $(\alpha_{cr}, \varepsilon_{cr}, \theta_{cr})$ thus found defines the critical point.

DISCUSSION OF RESULTS AND COMPARISON WITH TEST DATA

The experimental study was conducted on specimens made of 15 plies of unidirectional (0^0 angle ply) prepreg Kevlar 49 of the following specifications: commercial type SP-328, nominal thickness per ply 0·20 mm (0·008 in), nominal stiffness $E = E_1 = 75{\cdot}8$ GPa (11×10^6 psi), $E_2 = 5{\cdot}5$ GPa ($0{\cdot}8 \times 10^6$ psi), $G_{12} = 2{\cdot}1$ GPa ($0{\cdot}3 \times 10^6$ psi), Poisson's ratio $\nu_{12} = 0{\cdot}34$. A delamination of length $l = 50{\cdot}8$ mm (2 in) was introduced by a Teflon strip of

TABLE 1
Snap-Buckling Load

H/T	M_{0cr} (*N m*) *from theory*	M_{0cr} (*N m*) *from tests*
1/15	0·45	0·30
3/15	5·03	4·50
4/15	10·46	9·80

0·025 mm (0·001 in) thickness placed in the middle of the length. In this study, the delamination was introduced through the width and at specific locations through the thickness (between plies), resulting in a certain range of H/T values. A width of 12·7 mm (0·5 in) was used. The specimens had a length of 152·4 mm (6 in) and the distance between the outer and inner load points (moment arm) was 25·4 mm (1 in), whereas the distance between the two inner load points was 63·5 mm (2·5 in).

Four-point bending tests were performed in a 9 metric tonne (20 kip) MTS servo-hydraulic machine. They were carried out on stroke control with a rate of about 0·2 mm s^{-1}. Strain gages were placed at the middle of the delaminated layer so that the point of snap buckling can be determined from the sign reversal of the strain. Load-deflection and strain-deflection curves were obtained.

Table 1 shows the values of the critical bending moment M_0, as predicted from the theory, and as obtained from the experiments. The agreement is reasonable, with the experimental load being, in general, lower. Figure 2 shows the applied moment, M_0, and strain at the middle of the delaminated layer vs the crosshead displacement, δ, for the case of delaminated layer

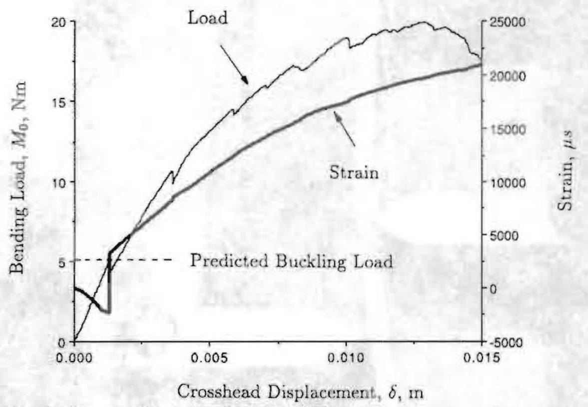

Fig. 2. Bending load, M_0, and strain at the middle of the upper delaminated layer vs applied crosshead displacement, δ. The level of the predicted snap-buckling load is also indicated. The data is for a Kevlar/epoxy specimen with $H/T = 3/15$.

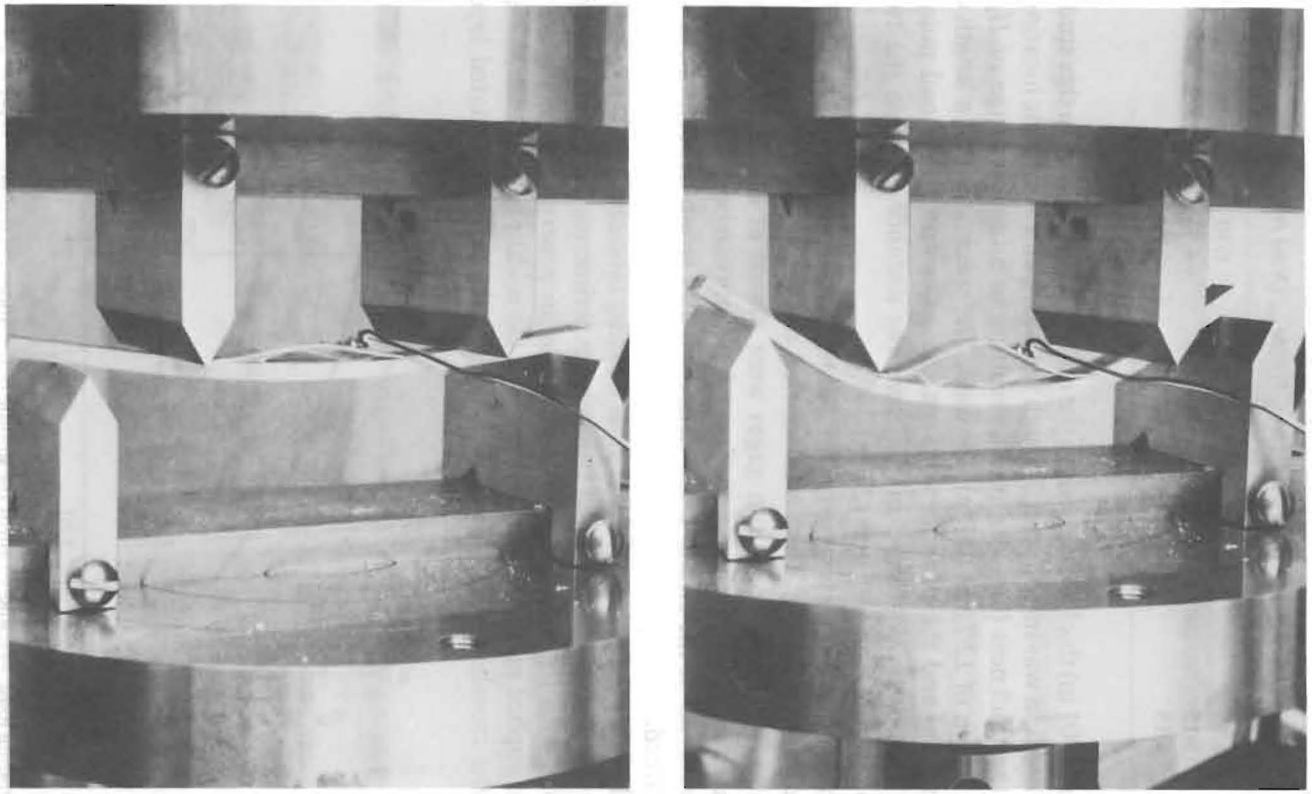

(a) (b)

Fig. 3. State of deformation for the specimen of Fig. 2, at the point of applied bending load (a) $M_0 = 10{\cdot}4$ N m and (b) $M_0 = 17{\cdot}1$ N m.

thickness $H/T = 3/15$. Snap buckling occurs at the point where the strain changes sign. The level of the predicted theoretical buckling load is also indicated, and is seen to be close to the experimentally obtained snap buckling load.

Finally, Fig. 3 illustrates the snap-buckling phenomenon and shows the state of deformation of the specimen whose load–deflection and strain–deflection curves are in Fig. 2, for applied bending load of (a) $M_0 = 10{\cdot}4$ N m and (b) $M_0 = 17{\cdot}1$ N m. It should be noted that, for this specimen, the snap-buckling load is at about $M_{0_{cr}} = 4{\cdot}5$ N m (Fig. 2). Moderate amounts of deflections are seen to occur.

ACKNOWLEDGEMENTS

The support of GTRI, Contract E16-A10 is gratefully acknowledged. The experiments reported were carried out while the author was at General Motors Research Laboratories, Engineering Mechanics Department. The author is grateful to Dr Larry Howell, Department Head, for his interest and support.

REFERENCES

1. Johnson, W. & Ghosh, S. K., Some physical defects arising in composite material fabrication. *J. Mater. Sci.*, **16** (1981) 285–301.
2. Dorey, G., Impact damage in composites–development, consequences and prevention. In *Proceedings ICCM-VI, ECCM-2*, Vol. 3, Elsevier Applied Science, London, 1987, pp. 1–26.
3. Chai, H., Babcock, C. D. & Knauss, W. G., One-dimensional modelling of failure in laminated plates by delamination buckling. *Int. J. Solids Structures*, **17** (1981) 1069–83.
4. Yin, W.-L., Sallam, S. N. & Simitses, G. J., Ultimate axial load capacity of a delaminated beam–plate. *AIAA J.*, **24** (1986) 123–8.
5. Kardomateas, G. A. & Schmueser, D. W., Buckling and postbuckling of delaminated composites under compressive loads including transverse shear effects. *AIAA J.*, **26** (1988) 337–43.
6. Kardomateas, G. A., Large deformation effects in the postbuckling behavior of composites with thin delaminations. *AIAA J.*, **27** (1989) 624–31.
7. Wang, S. S., Zahlan, N. M. & Suemasu, H., Compressive stability of delaminated random short-fiber composites. Part I—Modeling and methods of analysis. *J. Comp. Mat.*, **19** (1985) 296–316.
8. Wang, S. S., Zahlan, N. M. & Suemasu, H., Compressive stability of delaminated random short-fiber composites. Part II—Experimental and analytical results. *J. Comp. Mat.*, **19** (1985) 317–33.

9. Chai, H. & Babcock, C. D., Two-dimensional modelling of compressive failure in delaminated laminates. *J. Comp. Mat.*, **19** (1985) 67–97.
10. Yin, W. L., Cylindrical buckling of laminated and delaminated plates. In *Proceedings, 27th SDM AIAA/ASME/ASCE/AHS Conference*, Paper 86-0883, San Antonio, TX, 1986, pp. 165–79.
11. Fei, Z. & Yin, W. L., Postbuckling growth of a circular delamination in a plate under axisymmetric compression and bending. In *Proceedings, 12th Southeastern Conference on Theoretical and Applied Mechanics (SECTAM XII)*, Pine Mountain, GA, 1984, pp. 130–4.
12. Gjelsvik, A. & Bodner, S. R., The energy criterion and snap buckling of arches. *Journal of the Engineering Mechanics Division, ASCE*, **88**(5) (1962) 87–134.
13. Gjelsvik, A. & Bodner, S. R., Nonsymmetrical snap buckling of spherical caps. *Journal of the Engineering Mechanics Division, ASCE*, **88**(5) (1962) 135–65.
14. Friedrichs, K. O., On the minimum buckling load for spherical shells. In *Von Kármán Anniversary Volume*. California Institute of Technology, Pasadena, CA, 1941, p. 258.
15. Britvek, S. J., *The Stability of Elastic Systems*. Pergamon, New York, 1973.